Casein kinase II promotes target silencing by miRISC through direct phosphorylation of the DEAD-box RNA helicase CGH-1

Amelia F. Alessi[a,b,1,2], Vishal Khivansara[a,2,3], Ting Han[a,2,4], Mallory A. Freeberg[a,c,1], James J. Moresco[d], Patricia G. Tu[d], Eric Montoye[e], John R. Yates III[d], Xantha Karp[e], and John K. Kim[a,b,1,5]

[a]Life Sciences Institute, University of Michigan, Ann Arbor, MI 48109; [b]Department of Human Genetics, University of Michigan, Ann Arbor, MI 48109; [c]Department of Computational Medicine and Bioinformatics, University of Michigan, Ann Arbor, MI 48109; [d]Department of Chemical Physiology, The Scripps Research Institute, La Jolla, CA 92037; and [e]Department of Biology, Central Michigan University, Mount Pleasant, MI 48859

Edited by Gary Ruvkun, Massachusetts General Hospital, Boston, MA, and approved November 17, 2015 (received for review May 15, 2015)

MicroRNAs (miRNAs) play essential, conserved roles in diverse developmental processes through association with the miRNA-induced silencing complex (miRISC). Whereas fundamental insights into the mechanistic framework of miRNA biogenesis and target gene silencing have been established, posttranslational modifications that affect miRISC function are less well understood. Here we report that the conserved serine/threonine kinase, casein kinase II (CK2), promotes miRISC function in *Caenorhabditis elegans*. CK2 inactivation results in developmental defects that phenocopy loss of miRISC cofactors and enhances the loss of miRNA function in diverse cellular contexts. Whereas CK2 is dispensable for miRNA biogenesis and the stability of miRISC cofactors, it is required for efficient miRISC target mRNA binding and silencing. Importantly, we identify the conserved DEAD-box RNA helicase, CGH-1/DDX6, as a key CK2 substrate within miRISC and demonstrate phosphorylation of a conserved N-terminal serine is required for CGH-1 function in the miRNA pathway.

microRNA | casein kinase II | phosphorylation | miRISC | CGH-1

Since the discovery of *lin-4* and *let-7* in *Caenorhabditis elegans*, microRNAs (miRNAs) have emerged as an evolutionarily conserved superfamily of small endogenous RNAs critical for posttranscriptional gene regulation (1, 2). miRNAs regulate diverse biological processes including animal development, cell differentiation, apoptosis, and metabolism (1–3). To date, at least 250 miRNAs have been identified in *C. elegans* and almost 10 times as many in human (4). Furthermore, miRNAs are predicted to target as much as half of the transcriptome, further underscoring their central role in posttranscriptional gene silencing mechanisms (5).

miRNAs are typically transcribed as long primary transcripts that are processed sequentially by the RNase III enzymes Drosha and Dicer to produce an ∼70-nt precursor hairpin and an ∼22-nt RNA duplex, respectively (6, 7). One strand of the duplex is selectively loaded as the mature miRNA into an Argonaute (Ago) family protein that forms the core of miRNA-induced silencing complex (miRISC) in conjunction with a GW182 family protein (6, 7). Partial base pairing of the miRNA with complementary sites predominantly located in the 3′UTR of target mRNAs leads to transcript destabilization, translational repression, or both (3, 8).

Through a combination of genetic and biochemical approaches, conserved miRISC factors have been identified in *C. elegans*, including Argonaute-like genes ALG-1 and ALG-2, orthologs of human Ago2 (9). Mutation of *alg-1* results in pleiotropic phenotypes, consistent with loss of miRNA regulation in diverse biological pathways (9, 10). In contrast, *alg-2* mutants are superficially wild type, suggesting a partially redundant role in miRNA-mediated processes (10). ALG-1 physically interacts with AIN-1 and AIN-2 (ALG-1 interacting protein), functional orthologs of human GW182 (11, 12). AIN-1/2 are required for the localization of ALG-1 to processing bodies (P bodies), major cytoplasmic centers for mRNA catabolism and storage. Thus, AIN-1/2 functions as a molecular link between target-bound miRISC and downstream machinery required for translational repression and degradation of target mRNAs (11, 12).

Activity of miRISC is facilitated by conserved cofactors that include the DEAD-box RNA helicase CGH-1 and the TRIM-NHL ubiquitin ligase NHL-2. CGH-1 and its homologs are broadly involved in regulating mRNA stability and translation during development and differentiation in both somatic and germ cells (13, 14). In *C. elegans*, *cgh-1* and *nhl-2* are required for effective miRISC target silencing (15). The human ortholog of CGH-1, DDX6, has been shown to promote miRISC by interaction with the CCR4-NOT deadenylase complex and mRNA degradation machinery (16–18). The *C. elegans* miRISC also

Significance

MicroRNAs (miRNAs) are critical regulators of diverse biological processes. Despite rapid advances in understanding miRNA biogenesis and function, a gap remains in our knowledge of how miRNA effector complex activity [miRNA-induced silencing complex (miRISC)] is modulated. Specifically, the importance of posttranslational protein modifications in controlling miRISC activity remains largely unexplored. Here, we characterize a previously unidentified role for the conserved serine/threonine kinase, casein kinase II (CK2), in promoting the miRNA pathway in *Caenorhabditis elegans*. Notably, we establish the requirement of CK2 for miRNA function and provide mechanistic evidence that loss of CK2 compromises miRISC binding to mRNA targets. Furthermore, we identify that the miRISC cofactor and DEAD-box RNA helicase, CGH-1/DDX6, is phosphorylated by CK2 at a conserved residue, which is required for CGH-1–mediated miRNA function.

Author contributions: A.F.A., T.H., X.K., and J.K.K. designed research; A.F.A., V.K., T.H., J.J.M., P.G.T., E.M., J.R.Y., and X.K. performed research; M.A.F. analyzed data; and A.F.A., T.H., and J.K.K. wrote the paper.

The authors declare no conflict of interest.

This article is a PNAS Direct Submission.

Freely available online through the PNAS open access option.

Data deposition: The data reported in this paper have been deposited in the Gene Expression Omnibus (GEO) database, www.ncbi.nlm.nih.gov/geo (accession no. GSE66764).

[1]Present address: Department of Biology, Johns Hopkins University, Baltimore, MD 21218.

[2]A.F.A., V.K., and T.H. contributed equally to this work.

[3]Present address: Children's Research Institute, Department of Pediatrics, UT Southwestern Medical Center, Dallas, TX 75390.

[4]Present address: Department of Biochemistry, UT Southwestern Medical Center, Dallas, TX 75390.

[5]To whom correspondence should be addressed. Email: jnkim@jhu.edu.

This article contains supporting information online at www.pnas.org/lookup/suppl/doi:10.1073/pnas.1509499112/-/DCSupplemental.

contains the fly Vasa Intronic Gene ortholog, VIG-1, and the Tudor domain protein, TSN-1, that have both been shown to be required for silencing of a let-7 target 3′UTR reporter (19).

Posttranslational modifications (PTMs) have recently emerged as a potential mechanism for directly regulating miRISC activity (20). To date, a limited number of studies have addressed the functional role of PTMs of miRNA pathway machinery. In particular, several PTMs to Argonaute have been characterized (21–30). However, little is known about the identity and functional significance PTMs in other components of miRISC.

Previously, we reported the identification of several signaling kinases, including the conserved serine/threonine kinase, casein kinase II (CK2), in a genome-wide RNAi screen for candidate factors involved in small RNA-mediated silencing in *C. elegans* (31, 32). In this study, we characterize the role of CK2 as a positive regulator of miRISC activity in *C. elegans*. We provide evidence that CK2 functions downstream of miRNA biogenesis and is necessary for efficient miRISC binding to target mRNAs. Furthermore, we demonstrate that CK2 is required for phosphorylation of the miRISC cofactor CGH-1, which was previously implicated in facilitating miRISC-target interactions (15). Our data indicate that CK2 phosphorylation of CGH-1 at a conserved serine residue within an N-terminal CK2 motif is required for CGH-1 function in developmental pathways regulated by miRNAs.

Results

The CK2 holoenzyme consists of two catalytic α subunits and two regulatory β subunits in a tetrameric α2β2 configuration (33). In *C. elegans*, *kin-3* and *kin-10* encode the catalytic and regulatory subunits of CK2, respectively (34). In addition to identifying *kin-10* in a genome-wide screen for factors required for RNAi (31), we identified both CK2 subunits among factors that coimmunopurified with the GW182 homolog, AIN-1, by liquid chromatography coupled with tandem mass spectrometry. In addition to other core miRISC factors (ALG-1, ALG-2, and CGH-1), we recovered one KIN-3 peptide (KVLGTDELYEYIARY; 3.6% sequence coverage) and two KIN-10 peptides (RGNEFFCEVDEEYIQDRF and RFNLTGLNEQVPKY; 12% sequence coverage) that were absent in proteins immunopurified from the *ain-1*(*tm3681*) mutant (*SI Appendix*, Table S1), suggesting that CK2 physically interacts with miRISC.

CK2 Facilitates miRNA-Dependent Adult Hypodermal Remodeling. The first miRNAs were characterized as factors with altered timing of specific developmental events, including hypodermal remodeling (1, 2). During postembryonic development, *C. elegans* proceeds through four larval stages (L1–L4) before emerging as an adult. Loss of core miRISC factors results in reiteration of larval developmental patterns and failure or delay in the initiation of adult-specific programs. To investigate if CK2 regulates the miRNA pathway, we first analyzed animals depleted of *kin-3* or *kin-10* for phenotypes associated with compromised miRISC function in the hypodermis. Because CK2 is essential for viability, we used *kin-3* and *kin-10* RNAi (hereafter referred to as CK2 RNAi) to attenuate its expression (*SI Appendix*, Fig. S1 *A* and *B*). The formation of cuticle protrusions, termed alae, along the left and right sides of the adult animal requires the *let-7* family of miRNAs (1, 35). To investigate whether CK2 was required for the proper formation of adult alae, we compared alae formation in animals fed *kin-3* and *kin-10* RNAi to empty vector control RNAi. Whereas wild-type animals on empty vector control RNAi display no alae defects, RNAi of CK2 results in penetrant adult alae defects similar to those observed in RNAi of *alg-1*, which encodes the primary Argonaute protein in miRISC (Fig. 1*A*). Similarly, seam cells are generated through stem-cell–like divisions during larval transitions, terminally differentiating in the adult to yield 16 laterally distributed seam cells on each side of the body (36) that can be visualized using a seam-cell–specific GFP reporter (37). Whereas wild-type animals invariably have 16 seam cells, animals subjected to CK2 RNAi exhibit significantly increased numbers of seam cells, similar to animals depleted of miRISC components ALG-1, AIN-1, or NHL-2 (Fig. 1*B*). These data indicate that CK2 is required for appropriate seam cell differentiation. Finally, we examined the timing of expression of a GFP reporter for the adult-specific collagen, COL-19, whose expression is controlled by miRNAs that regulate the heterochronic pathway (38, 39). Whereas ≤5% of animals on empty vector control RNAi fail to express P*col-19::gfp* expression at three separate time points during adulthood, 20–35% of adult animals on CK2 RNAi consistently lack GFP reporter expression even at the terminal gravid adult stage examined, which is comparable to depletion of the core miRISC factor *ain-1* (*SI Appendix*, Fig. S2*A*). Taken together, these results indicate that loss of CK2 phenocopies loss of miRISC components, which suggests CK2 facilitates miRNA-mediated adult hypodermal remodeling during the larval-to-adult transition.

CK2 Promotes *let-7* miRNA Family and miRISC Function. To further define the role of CK2 in the miRNA pathway, we examined genetic interactions between CK2 and *let-7* family miRNAs and miRISC components. Mild phenotypes elicited by hypomorphic mutations in miRNA pathway genes create sensitized genetic backgrounds that can be enhanced by mutations in other genes required for the pathway. Therefore, we examined whether loss of *kin-3* or *kin-10* could enhance phenotypes associated with hypomorphic mutations in genes of the miRNA pathway.

In the transition period between each larval stage, *C. elegans* proceed through a quiescent state called lethargus, where animals cease pharyngeal pumping and reduce locomotion before molting. In retarded heterochronic mutants, lethargus is reiterated at the adult stage (1, 35, 40). A mutant for *mir-48*, a member of the *let-7* family of miRNAs, exhibits a low level of adult lethargus that is exacerbated by deleting its paralog, *mir-84* (35) (Fig. 1*C*). In the *mir-48*(*n4097*) sensitized genetic background, adult lethargus is significantly enhanced by CK2 RNAi at levels comparable to RNAi of miRISC components (Fig. 1*C*). CK2 RNAi did not affect lethargus in wild-type animals (*SI Appendix*, Table S2). Likewise, loss of *let-7* activity leads to a rupturing (Rup) phenotype, in which animals herniate through the vulva and subsequently die (1). Two hypomorphic *let-7* alleles (*mg279* and *n2853*) exhibit a mild Rup phenotype, which is enhanced by CK2 RNAi at levels comparable to RNAi of miRISC components (Fig. 1*D*). *let-7* family mutants, *mir-48*(*n4097*) and the *mir-48*(*n4097*); *mir-84*(*n4037*) double mutant (35), as well as core miRISC factor mutants, *alg-1*(*tm369*) and *ain-1*(*ku322*) (9, 12) also display Rup phenotypes that are exacerbated by CK2 RNAi (Fig. 1*D*). Together these data suggest loss of CK2 enhances mutant phenotypes of the *let-7* family of miRNAs.

To rule out the possibility of off-target effects of RNAi, we confirmed enhancement of *let-7* mutant phenotypes in *kin-10* deletion mutants. CK2 is essential for *C. elegans* development: *kin-3* (−/−) null mutants arrest as L3 larvae and *kin-10* (−/−) as L4 larvae. Consequently, CK2 null mutants are maintained in a genetically balanced background. Because the Rup phenotype can only be assessed in animals that reach the L4 stage, we examined two deletion mutants of *kin-10* (*ok1751* and *ok2031*) in the sensitized *let-7*(*mg279*) background. Consistent with results using *kin-10* RNAi, we observe an enhanced Rup phenotype in *kin-10* (−/−) relative to the balanced *kin-10* (+/−) siblings for both *kin-10* alleles (Fig. 1*E*). Importantly, these data indicate that *kin-10* genetic mutants recapitulate *kin-10* RNAi phenotypes.

Rup phenotypes of *let-7* family mutants can be partially suppressed by concurrent depletion of their mRNA targets (35, 41).

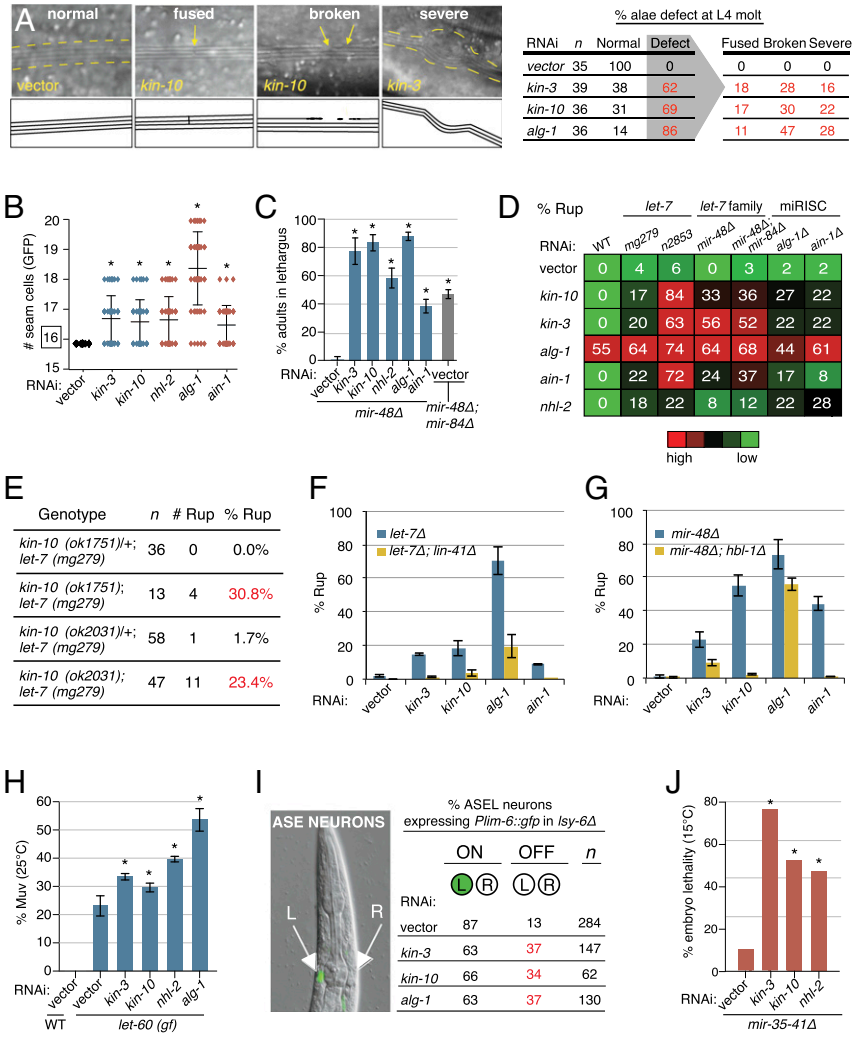

Fig. 1. CK2 genetically interacts with the miRNA pathway. (*A* and *B*) CK2 depletion results in phenotypes associated with reduced miRNA pathway function. (*A*) RNAi of *kin-3*, *kin-10*, or *alg-1* significantly increases defective alae versus empty vector control (two-tailed Fisher's exact test $P < 0.0001$). (*B*) RNAi of *kin-3*, *kin-10*, *nhl-2*, *alg-1*, and *ain-1* in animals expressing a seam cell gfp reporter *(Pscm::gfp)* all exhibit significant seam cell hyperplasia post-L4 versus empty vector control (two-tailed Student's *t* test $*P < 0.001$, mean and SD plotted, $n = 50$). (*C*–*J*) CK2 depletion enhances miRNA mutant defects. (*C*) RNAi of *kin-3*, *kin-10*, *nhl-2*, *alg-1*, and *ain-1* all exhibit significant enhancement of adult animals in lethargus versus empty vector control (two-tailed Student's *t* test of biological replicates $*P < 0.05$, mean and SD plotted, $n \geq 50$ per replicate). Adult animals inappropriately entering lethargus were scored every 2 h from 60 h to 72 h post-L1. (*D*) *kin-3* and *kin-10* RNAi enhance Rup of *let-7*, *let-7* family, and miRISC factor mutants at 72 h post-L1 (20 °C). Heatmap represents mean percent Rup of biological replicates ($n \geq 50$ per replicate). (*E*) Rup in homozygous *kin-10* deletion mutants is significantly greater than *hT2[qIs48]* balanced *kin-10*/+ siblings (two-tailed Fisher's exact test $P \leq 0.003$). (*F* and *G*) *kin-3* and *kin-10* RNAi Rup enhancement in *let-7* and *mir-48* mutants is dependent on their targets. (*F*) Rup enhancement of *kin-3 and kin-10* RNAi in *let-7*(*mg279*) is decreased in the *lin-41*(*ma104*) background (mean and SD of biological replicates plotted, $n \geq 37$ per replicate). (*G*) Rup enhancement of *kin-3* and *kin-10* RNAi in *mir-48*(*n4097*) is decreased in the *hbl-1*(*mg285*) background (mean and SD of biological replicates, $n \geq 56$ per replicate). (*H*) RNAi of *kin-3*, *kin-10*, *nhl-2*, and *alg-1* all significantly enhance Muv versus empty vector control (two-tailed Student's *t* test of biological replicates $*P < 0.05$, mean and SD plotted, $n \geq 94$ per replicate). (*I*) *kin-3* and *kin-10* RNAi increase the penetrance of ASEL misspecification in neuronal RNAi-competent *lsy-6*(*ot150*) strain indicated by the lack of P*lim-6*::*gfp* expression in ASEL (Fisher's exact test $P < 0.0001$ for *kin-3* and *alg-1* RNAi, $P = 0.0002$ for *kin-10* RNAi). (*J*) *kin-3* and *kin-10* RNAi enhance embryonic lethality in *mir-35-41*(*nDf50*) (two-tailed Fisher's exact test $*P < 0.001$, $n \geq 145$).

Consistent with the hypothesis that CK2 promotes miRISC-mediated target silencing, Rup enhancement by CK2 RNAi in the *let-7* and *miR-48* mutants is suppressed by hypomorphic mutations in their respective targets, *lin-41* and *hbl-1* (Fig. 1 *F* and *G*). *miR-84* also regulates vulval precursor cell (VPC) fate specification by attenuating the expression of its target *let-60*/*RAS* (42, 43). Failure to repress LET-60 activity in specific VPCs leads to vulval cell misspecification and a multivulva phenotype (Muv) (42). CK2 RNAi enhances Muv in a mild gain-of-function *let-60*(*ga89*) allele (44) (Fig. 1*H*). Taken together, these data indicate that CK2 genetically interacts with the *let-7* family of miRNAs to promote miRISC function in a target-dependent manner.

CK2 Is Required for the Function of lsy-6 and miR-35 Family miRNAs. Because CK2 is broadly expressed (*SI Appendix*, Fig. S2*B*), we tested whether it is required for the function of non–*let-7* family miRNAs. The miRNA lsy-6 functions to specify the fate of ASEL, one of two morphologically similar, bilaterally symmetric ASE neurons (ASEL and ASER), which can be monitored by expression of an ASEL-specific P*lim-6*::*gfp* reporter (45). Because many neurons in *C. elegans* are refractory to RNAi (46), we performed RNAi experiments in an *nre-1* mutant background, which potentiates RNAi-mediated gene silencing in neurons (47). CK2 RNAi enhances the penetrance of ASEL misspecification in the *lsy-6*(*ot150*) hypomorph (48) to the same

extent as *alg-1* RNAi (Fig. 1*I*), indicating that CK2 promotes lsy-6 function.

The miR-35 family of miRNAs (miR-35–42) is expressed during embryogenesis and functions redundantly to control embryonic development (49). Deletion of *mir-35–41* leads to semipenetrant, temperature-sensitive late embryonic lethality (49). At the permissive temperature (15 °C), ∼10% of embryos display this phenotype, whereas the remaining 90% develop normally. Depletion of CK2 or the gene encoding the core miRISC factor *nhl-2* significantly increases embryonic lethality, consistent with the requirement of CK2 for the function of the miR-35 family of miRNAs (Fig. 1*J*). In contrast, loss of CK2 does not enhance the low level of embryonic lethality in wild-type animals (*SI Appendix*, Table S3). Collectively, our results are consistent with CK2 broadly promoting miRNA function to mediate a range of biological processes in multiple *C. elegans* tissues.

CK2 Is Required for miRNA Target Silencing. Because KIN-3 and KIN-10 depletion enhances multiple miRNA mutant phenotypes, we sought to determine whether these CK2-dependent physiological defects could be explained by miRNA target derepression. We examined the endogenous, developmentally regulated targets of both let-7 family and lin-4 miRNAs (Fig. 2*A*). In *C. elegans*, let-7 triggers the rapid degradation of *lin-41* mRNA at the L4-to-adult transition (50, 51). *lin-41* encodes a TRIM/RBCC family protein, homologous to human TRIM71 (52), that negatively regulates expression of LIN-29, a transcription factor required for adult cell fate specification (50). Depletion of *alg-1* leads to significant derepression of *lin-41* mRNA compared with empty vector RNAi (Fig. 2*B*). Similarly, knockdown of CK2 also significantly derepresses *lin-41* levels by 1.5- to 2-fold (Fig. 2*B*, *Left*). Significant derepression is also observed for the let-7 family target, *daf-12*, which encodes a nuclear steroid hormone receptor that integrates environmental signals and developmental timing (51, 53) (Fig. 2*B*, *Right*).

To determine whether derepression of target mRNAs by CK2 RNAi results in elevated target mRNA translation, we examined endogenous protein levels of LIN-14 upon CK2 RNAi. The early-acting heterochronic miRNA, lin-4, targets and silences *lin-14* mRNA during the L1-to-L2 larval transition (2, 54), resulting in a commensurate decrease in LIN-14 protein. In animals fed empty vector control RNAi, the LIN-14 protein is robustly expressed during the L1 stage (4 h) and dramatically decreases by the L2 stage (Fig. 2*C*, 20 h). In contrast, when animals are subjected to CK2 RNAi, LIN-14 levels remain high during the L1-to-L2 transition to a similar degree as, or possibly higher than, animals on *alg-1* RNAi (Fig. 2*C*, 16- to 20-h time points). The elevated LIN-14 expression is not due to any dramatic developmental delay caused by CK2 or *alg-1* RNAi during this time frame based on measurements of animal growth (*SI Appendix*, Fig. S3).

Next we examined miR-1–dependent silencing of *mef-2*, which encodes a muscle-specific transcription factor (55), using a 3′ UTR GFP reporter driven by the muscle-specific *myo-3* promoter (Fig. 2*D*). Image analysis suggests that depletion of *kin-3*, *kin-10*, or *alg-1* significantly increases the intensity of *mef-2* reporter expression compared with empty vector RNAi (Fig. 2 *D* and *E*). To test the miR-1 dependence of target reporter expression, we scrambled the two miR-1 binding sites in the *mef-2* 3′ UTR. Consistent with a miR-1–dependent effect, no significant difference in GFP expression was detected in the scrambled reporter with CK2 or *alg-1* RNAi versus empty vector control (Fig. 2 *D* and *E*). Taken together, our genetic and target expression data indicate that CK2 promotes miRNA-mediated target silencing in a wide array of tissues and developmental stages.

CK2 Is Dispensable for the Expression of miRNAs and miRISC Factors. To explore where in the miRNA pathway CK2 functions, we first investigated whether CK2 regulates the biogenesis or stability of mature miRNAs. We performed deep sequencing of small RNAs in wild-type animals treated with vector, *kin-3*, or *kin-10* RNAi and observed no significant differences in the global levels of mature miRNAs between empty vector and CK2 RNAi (Fig. 3*A* and *SI Appendix*, Fig. S4*A* and Table S4). Furthermore, Northern blot analysis of miR-48, miR-1, and *bantam* miRNA family ortholog, miR-58, in wild-type and sensitized *alg-1*(*tm369*) animals confirmed that CK2 RNAi does not dramatically affect mature or precursor miRNA levels (Fig. 3*B* and *SI Appendix*, Fig. S4 *B* and *C*). We also examined whether CK2 regulates the accumulation or stability of core miRISC proteins. We detect no difference by Western blot of endogenous ALG-1, AIN-1, VIG-1, TSN-1, and CGH-1 levels between empty vector and CK2 RNAi (Fig. 3*C*). Together, these data indicate that CK2 functions downstream of miRNA biogenesis and is not required for stability and/or expression of individual miRISC factors.

CK2 Promotes miRISC Association with mRNA Targets. Defects in miRISC target silencing could result from compromised ability to bind mature miRNAs or mRNA targets. To determine whether CK2 is required for miRNA or target binding to miRISC, we performed RNA immunoprecipitation (RIP) using a strain expressing GFP::ALG-1 (56) and compared relative miRNA and target mRNA binding in CK2 RNAi versus empty vector and *gfp* RNAi controls (Fig. 3*D*). We observed no significant differences in the levels of let-7 or miR-48 associated with miRISC upon CK2 RNAi versus empty vector control RNAi (Fig. 3*E*). Importantly, the target mRNAs of these miRNAs, *lin-41* and *daf-12*, show an approximately twofold reduction in miRISC association upon CK2 RNAi (Fig. 3*F*) despite their global up-regulation (Fig. 2*B*). As expected, RNAi of *gfp*, which reduces the expression of GFP::ALG-1, exhibited significant reduction of both miRNA and target mRNA levels (Fig. 3 *F* and *G*). Taken together, these data indicate that CK2 promotes efficient binding of target mRNAs, but not mature miRNAs, to miRISC.

CK2 Phosphorylates miRISC Cofactor CGH-1. Given our mass spectrometry data that CK2 physically associates with miRISC, we hypothesized that CK2 promotes miRISC target binding by phosphorylating one or more miRISC cofactors. We queried a *C. elegans* phosphoproteome dataset (57) and found peptides phosphorylated at CK2 motifs in CGH-1 and VIG-1. Because *cgh-1* loss-of-function mutants display developmental phenotypes that are easy to observe and CGH-1 has been implicated in promoting miRISC-target interactions (15), we first examined whether CK2 physically interacts with CGH-1. Endogenous KIN-3 coimmunopurified with CGH-1::GFP in lysates from *C. elegans* fed *glp-1* RNAi to enrich the capture of interactions in somatic tissues, the major sites of miRNA-mediated gene regulation (Fig. 4*A*). *glp-1* encodes a *C. elegans* Notch family receptor (58) required for mitotic proliferation of germ cells and maintenance of germ-line stem cells (59). *glp-1* RNAi severely disrupts early germ-line development yielding adult animals that are primarily composed of somatic cells. Mass spectrometry of endogenous CGH-1 complexes confirmed the interaction of KIN-3 and additionally identified peptides corresponding to KIN-10 and other known CGH-1 interactors, including NHL-2 (*SI Appendix*, Table S5).

To establish whether CGH-1 could be phosphorylated by CK2, we performed in vitro kinase assays. CK2 phosphorylates full-length CGH-1 in a manner dependent on CK2 activity, as inhibition of CK2 by addition of the CK2 inhibitor, 4,5,6,7-tetrabromobenzotriazole (TBB), or use of a catalytically dead KIN-3 (K67M) abrogates CGH-1 phosphorylation (Fig. 4*B*).

CGH-1 harbors four sites matching the CK2 consensus phosphorylation motif ([S/T]-X-X-[D/E]) (Fig. 4*C*). In vitro kinase assays with short CGH-1 peptides containing each putative CK2 phosphorylation site indicate that site 1, containing serine 2 (S2), is the predominant site phosphorylated by CK2 (Fig. 4*D*). Phosphoproteomic analysis by mass spectrometry of immunopurified CGH-1 recovered peptides containing phosphorylated S2 from empty vector RNAi samples, but not *kin-3* RNAi samples, suggesting that site 1 is phosphorylated in vivo in a CK2-dependent manner (*SI Appendix*, Table S6). Whereas S2 is not located in any functionally annotated domain of CGH-1, it is within an N-terminal intrinsically disordered region (60) that is conserved in DDX6 (*SI Appendix*, Fig. S5). Intrinsically disordered regions have been hypothesized to be subject to posttranslational modifications by kinases and phosphatases, which may regulate protein function (25, 61). In addition, serine 2 of CGH-1 is broadly conserved in orthologous proteins and conservation of phosphorylation at this site is supported by large-scale phosphoproteomic evidence in amphibians and mammals (62, 63).

CK2 Phosphorylation of CGH-1 Promotes miRISC Function. If CK2 phosphorylation of CGH-1 at S2 is important for CGH-1 to

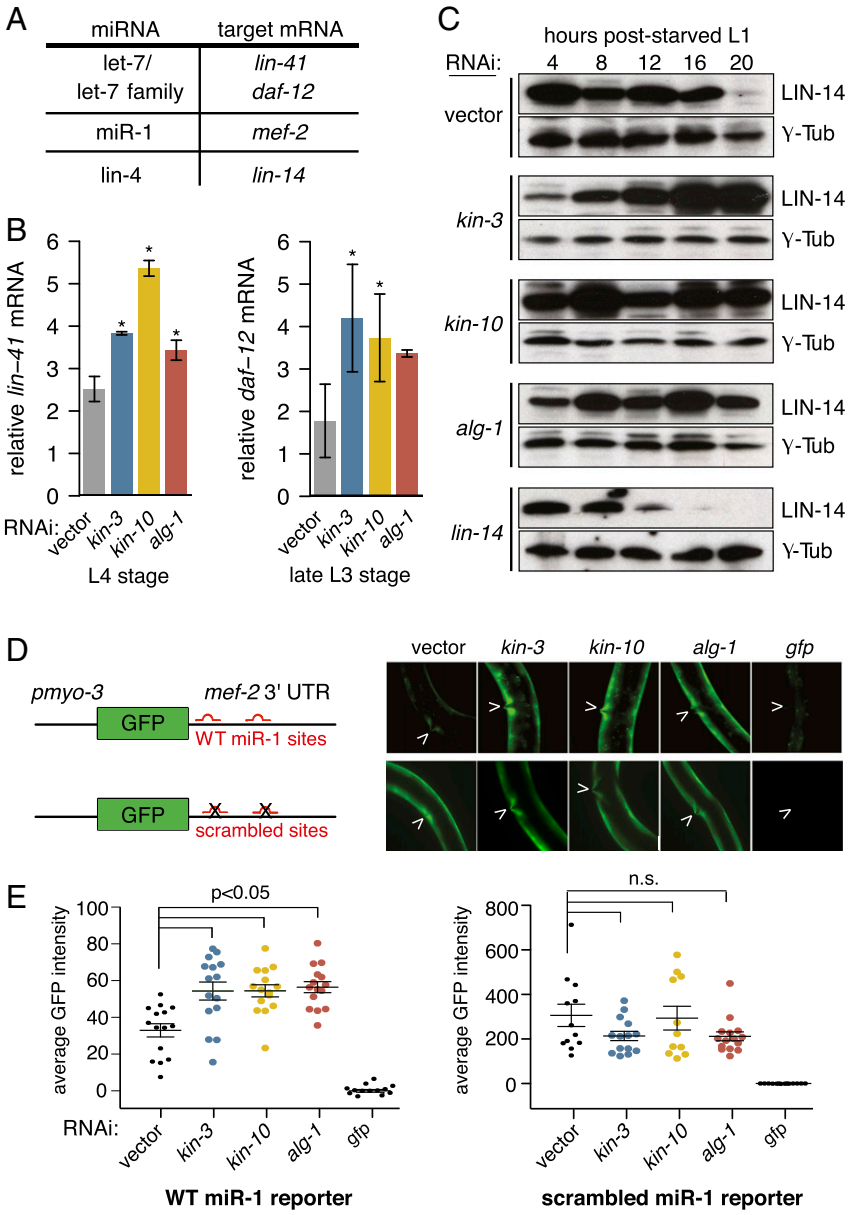

Fig. 2. CK2 is required for miRNA target silencing. (*A*) Abridged table of miRNAs and their target mRNAs examined in this study. (*B*) *kin-3 and kin-10* RNAi attenuate silencing of let-7 family targets *lin-41* and *daf-12*: *lin-41* mRNA levels are significantly elevated in *kin-3 and kin-10* RNAi versus vector RNAi (44 h post-L1, 20 °C) (*Left*); *daf-12* mRNA levels are significantly elevated in *kin-3 and kin-10* RNAi versus vector RNAi (40 h post-L1, 20 °C) (*Right*) (one-tailed Student's *t* test of two biological replicates for *lin-41* and three biological replicates for *daf-12*, $*P < 0.050$, mean and SD plotted). (*C*) *kin-3 and kin-10* RNAi attenuates silencing of *lin-4* target *lin-14*. LIN-14 is up-regulated in *kin-3* and *kin-10* RNAi versus empty vector control in L2 (16 h to 20 h post-L1). γ-Tubulin was used as a loading control. (*D* and *E*) *kin-3 and kin-10* RNAi attenuate silencing of miR-1 target *mef-2* in a miR-1–dependent manner. (*D*) Reporter constructs shown with wild-type and scrambled miR-1 sites (*Left*). Arrows indicate vulva in representative images (*Right*). (*E*) *mef-2* reporter quantification. RNAi of *kin-3*, *kin-10*, *and alg-1* all significantly increase GFP signal of the wild-type reporter versus vector ($P < 0.05$, mean and SD plotted, $n > 10$), but not the scrambled reporter ($P \geq 0.60$).

promote miRISC activity, then CGH-1 phosphorylation mutants should have altered miRISC function. To test this hypothesis, we generated multicopy CGH-1::GFP transgenic lines with phosphodefective (S2A) and phosphomimic (S2D/E) mutations (hereafter referred to as S2 variants). Multiple S2 variant lines were generated. Those with the most similar expression to wild-type *cgh-1::gfp* were selected for genetic analysis (*SI Appendix*, Fig. S6). Two phosphodefective lines are shown: S2A-2 has somatic expression levels most similar to the wild-type transgene (S2), whereas S2A-1 has substantially lower expression (*SI Appendix*, Fig. S6*A*). The phosphomimic S2D and S2E lines express at similar levels, which are slightly higher than the wild-type transgene (S2) (*SI Appendix*, Fig. S6*A*). Because *cgh-1* is critical in germ-line development and multicopy transgenes are commonly silenced in the *C. elegans* germ line, we examined the function of the S2 variants in the sensitized *let-7*(*mg279*) background using a temperature-sensitive *cgh-1* point mutant, *cgh-1*(*tn691*), which phenocopies *cgh-1* loss of function at the nonpermissive temperature of 25 °C (64). Alone, *cgh-1*(*tn691*); *let-7*(*mg279*) displays a partially penetrant protruding vulva phenotype (Pvul) that is significantly rescued by wild-type CGH-1::GFP expression (Fig. 4 *E* and *F*). Interestingly both phosphodefective lines significantly exacerbate Pvul despite the substantially lower expression of S2A-1 versus the wild-type trasngene (Fig. 4 *E* and *F*). Phosphomimics yielded fewer conclusive data: S2D mutants have a phenotype similar to the nontransgenic control, whereas S2E mutants show partial, but significant, rescue. We also examined the effect of the S2 variants on the retarded alae phenotype of *cgh-1*(*tn691*); *let-7*(*mg279*) mutants. Expression of wild-type and S2E CGH-1::GFP significantly rescues alae defects, whereas the phosphodefective S2A mutants and the S2D mutant have defects similar to, or greater than, the nontransgenic control (Fig. 4*G*). Thus, in two different tissues, the CGH-1 phosphodefective S2A mutation fails to complement miRNA mutant phenotypes. Based on the robust phenotype of the S2A mutants, we hypothesize that differential results with S2D and S2E may be attributed to incomplete phosphomimicry by the substituted amino acids. Together, these data support the hypothesis that phosphorylation at S2 is important for miRNA-dependent CGH-1 function.

To determine the requirement for CK2 and phosphorylation of CGH-1 in a biological context where miRNA activity is modulated, we compared continuous development to postdauer development. Continuous development from L1 to adulthood occurs in favorable environmental conditions. By contrast, adverse conditions promote entry into the stress-resistant and developmentally arrested dauer larval stage immediately after the L2 molt (65). If dauer larvae encounter an environment suitable for growth, they resume normal development such that postdauer cell divisions are identical to those occurring during continuous development (66, 67). Robustness to developmental

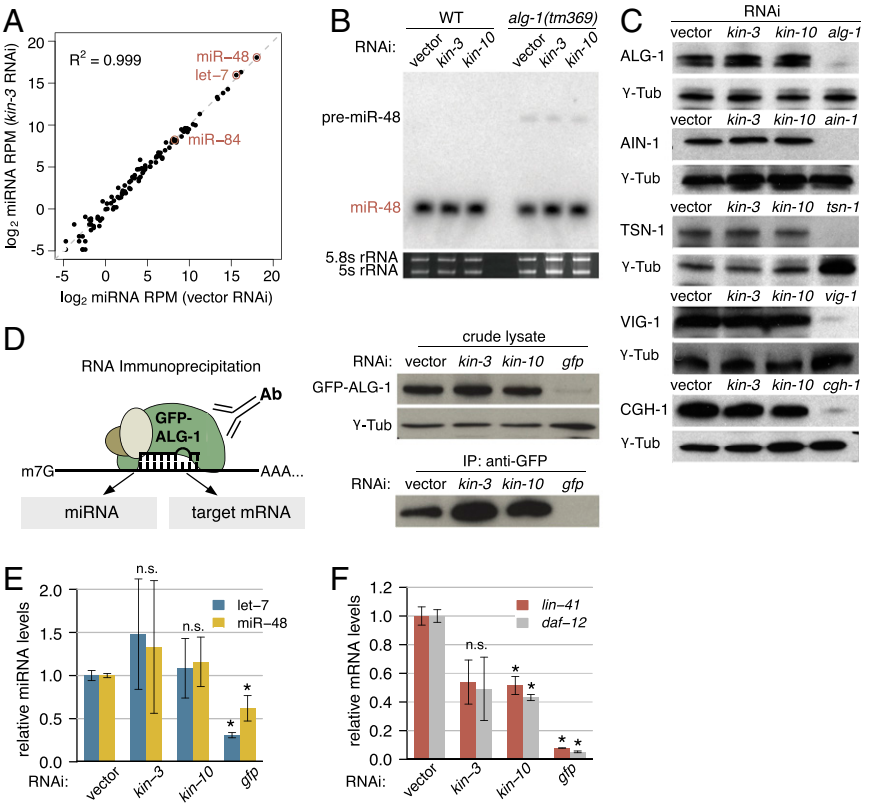

Fig. 3. CK2 promotes miRISC target binding. (*A* and *B*) CK2 does not affect miRNA levels. (*A*) *kin-3* RNAi does not affect global mature miRNA abundances as quantified by deep sequencing [reads per million (RPM) mapped reads]. (*B*) Global analysis in *A* is supported by Northern blotting: *kin-3* and *kin-10* RNAi do not substantially alter levels of precursor or mature miR-48 in wild-type or *alg-1*(*tm369*) animals. (*C*) CK2 RNAi does not considerably affect miRISC factor levels. Western analysis of core miRISC proteins in *kin-3* and *kin-10* RNAi are similar to empty vector control. (*D–F*) CK2 affects miRISC binding to target mRNAs. (*D*) Schematic and Western analysis of GFP::ALG-1 RNA immunoprecipitation (RIP) from L4 (48 h post-L1, 20 °C) lysates of empty vector versus *kin-3* and *kin-10* RNAi; *gfp* RNAi controls for RIP; γ-tubulin controls for protein input. (*E*) Levels of let-7 and miR-48 associated with GFP::ALG-1 are not significantly different in *kin-3* and *kin-10* RNAi versus empty vector. (*F*) Levels of *lin-41* and *daf-12* mRNA associated with GFP::ALG-1 are decreased in *kin-3* and *kin-10* RNAi versus empty vector. RIP RNAs were normalized to spiked-in Firefly Luciferase mRNA (one-tailed Student's *t* test of biological replicates $*P < 0.05$, mean and SD plotted).

interruption by dauer is due, in part, to enhanced activity of lin-4 and let-7 family miRNAs, such that lin-4 can substitute for miR-48, miR-241, and miR-84 during postdauer development but not continuous development (68). Surprisingly, enhancement of miRNA activity occurs without *alg-1*, as heterochronic phenotypes of *alg-1* mutants are efficiently suppressed postdauer (68). This suggests that modulatory proteins elevate the activity of the remaining ALG-2–containing miRISC. CK2 appears to contribute to this phenomenon, as *kin-3* RNAi significantly reduces postdauer suppression of *alg-1*(*gk214*) alae defects (*SI Appendix*, Fig. S7*A*). Interestingly, we observe that during postdauer development, the retarded alae phenotype of S2A mutants is significantly suppressed, suggesting that CK2 modification of CGH-1 is dispensable during postdauer development (*SI Appendix*, Fig. S7*B*).

Discussion

Here we report that subunits encoding the *C. elegans* casein kinase II, *kin-3* and *kin-10*, are required for effective activity of the miRNA pathway. Genetically, our analyses suggest that *kin-3* and *kin-10* promote the function of several miRNA/miRNA families that regulate diverse processes, including the conserved function of the *let-7* family of miRNAs in the control of animal development and cellular differentiation. Mechanistically, our analyses place CK2 function at the step of miRISC association with mRNA targets, downstream of miRNA biogenesis and loading into miRISC. Molecular assays indicate that CK2 subunits are required for target silencing and that their depletion compromises miRISC binding to let-7 target mRNAs. Through the use of proteomic and in vitro methods, we establish the conserved miRISC cofactor, CGH-1, as a direct CK2 substrate at a conserved N-terminal serine residue (S2). Additional genetic

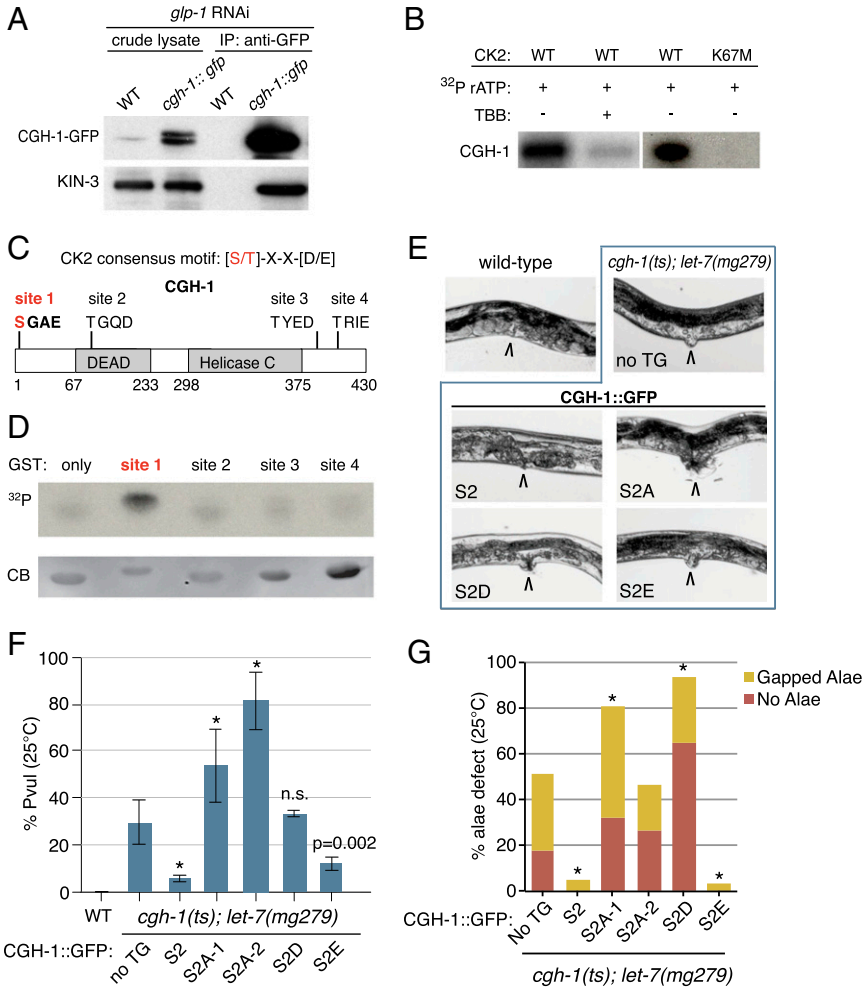

Fig. 4. CK2 phosphorylates miRISC factor CGH-1 at serine 2. (*A*) KIN-3 associates with CGH-1 in the soma. CK2 catalytic subunit, KIN-3, coimmunopurifies with CGH-1::GFP in L4 stage animals fed *glp-1* RNAi to prevent germ-line proliferation. (*B*) CGH-1 is phosphorylated by CK2 in vitro. Autoradiogram of GST-purified wild-type CGH-1 incubated with GST-purified CK2 composed of wild-type or ATP-binding site mutant KIN-3 (K67M). TBB, CK2 inhibitor (4,5,6,7-tetrabromobenzotriazole). (*C*) CGH-1 harbors four CK2 recognition motifs (sites 1–4). (*D*) Site 1 (serine 2) is phosphorylated by CK2 in vitro. GST-tagged CGH-1 peptides composed of 20 residues flanking each putative CK2 phosphorylation site were incubated in vitro with CK2 and analyzed by SDS/PAGE and autoradiography. ^{32}P, autoradiogram; CB, Coomassie Blue stained gel. (*E* and *F*) Genetic analysis of CGH-1 serine 2 (S2) phosphovariants in *cgh-1*(*tn691*)*ts; let-7*(*mg279*) suggests phosphorylation of CGH-1 at S2 promotes miRISC function (*E*) Representative images of Protruding vulva (Pvul). Adult vulva indicated by arrow (120 h post-L1, 25 °C). (*F*) Quantitation of Pvul. Compared with *cgh-1*(*tn691*)*ts; let-7*(*mg279*) with no transgene the *cgh-1::gfp* (S2) transgene significantly rescues Pvul. S2A mutants (lines 1 and 2) significantly enhance Pvul (two-tailed Fisher's exact test $*P < 0.0001$ for S2 variants versus "no TG," mean and SD plotted for three technical replicates within a single experiment, $n \geq 95$). (*G*) S2 and S2E significantly rescue alae defects of *cgh-1*(*tn691*)*ts; let-7*(*mg279*). S2A mutants significantly enhance (line 1) or have no significant effect (line 2) on defects (two-tailed Fisher's exact test $*P < 0.0001$ for S2 variants versus "no TG"). TG, transgene; S2A lines 1 and 2, phosphodefective Ser-to-Ala mutation; S2D/E, phosphomimic Ser-to-Asp/Glu mutations.

analyses suggest that S2 is important for miRNA-dependent CGH-1 function in the *let-7* pathway. Because CGH-1 is part of a family of DEAD-box RNA helicases that influence all permutations of protein–protein, protein–RNA, and RNA–RNA interactions, we propose that phosphorylation of CGH-1 by CK2 may influence miRISC target binding by (*i*) directly promoting miRISC interaction with targets, either by promoting CGH-1 association with miRISC or by altering affinity of a CGH-1–associated miRISC for targets, and/or (*ii*) promoting CGH-1 association with factors involved with mRNA translation and decay. Biochemically, phosphorylation in the N-terminal disordered region of CGH-1 may affect these changes by triggering a conformational change that alters the intrinsic activity of CGH-1 or facilitates its association with other factors.

Intriguingly, our analysis of postdauer development suggests that CK2 function in the *C. elegans* miRNA pathway is different from that during continuous development. Postdauer suppression of miRNA phenotypes requires CK2, but not CK2 phosphorylation of CGH-1 (*SI Appendix*, Fig. S7*B*), suggesting that during postdauer development, CK2 may have alternative miRNA pathway substrates. Alternatively, additional factors may dictate CK2 specificity during continuous development versus postdauer development. Despite considerable efforts, the matter of whether CK2 is constitutively active or activated by specific signals remains controversial (69). Therefore, further investigation into CK2 function in the miRNA pathway during postdauer development may prove a useful system for extending our understanding of the regulation of CK2. As modulating miRNA activity is crucial for development and disease, dissecting the mechanisms that activate or antagonize CK2 activity in the miRNA pathway may also provide further insights into how the miRNA pathway is regulated.

Ribonucleoprotein (RNP) granules, such as germ-line P granules and the miRISC-resident P bodies in somatic tissues, possess hydrogel-like properties (70, 71) whose dynamics of formation and dissolution depend, in part, on the phosphorylation of granule components. RNA binding proteins within these granules typically contain low complexity sequences at their N and C termini that form disordered domains (72). These regions are often sites for phosphorylation and other posttranslational modifications that trigger or inhibit the phase transition properties of RNA-binding proteins (73–76). Interestingly, the CK2 phosphorylation site on CGH-1 (and human DDX6) resides within a prominent disordered region in its N terminus. Furthermore, a recent study of germ-line P granules demonstrated that inactivation of CGH-1 in the germ line causes a profound transformation of P granules from a hydrogel-like state to a striking, rigid square-shaped matrix (70). Thus, we speculate that CK2-mediated phosphorylation of CGH-1 in somatic tissues, the predominant sites of miRNA-mediated gene regulation, may promote CGH-1 recruitment to miRISC-resident P bodies and possibly affect the recruitment of other cofactors to miRISC RNP granules.

Materials and Methods

Detailed methods are available in *SI Appendix, Supplemental Materials and Methods*.

***C. elegans* Strains and Plasmids.** All strains used in this study are listed in *SI Appendix*, Table S7. *C. elegans* were grown and maintained under standard laboratory conditions (77) and synchronized by hypochlorite treatment and overnight hatching in M9 buffer, except where indicated. Descriptions of plasmid construction and generation of transgenic animals are described in *SI Appendix, Supplemental Materials and Methods*.

RNAi. All RNAi clones are from the Ahringer RNAi library (78), except the *kin-3* RNAi clone, which is from the *C. elegans* ORFeome RNAi library (79), and the *cgh-1* 3′ UTR RNAi clone (pJK301), which was made for this study. Standard feeding RNAi procedures (80) were followed. Specific modifications to RNAi conditions, including duration, strength, and temperature, are detailed in *SI Appendix, Supplemental Materials and Methods*.

Pcol-19::gfp Phenotyping. The relative number of animals expressing GFP were tracked from young to gravid adulthood by scoring the number of animals expressing GFP at 60 h, 72 h, and 80 h post-L1 at 20 °C.

mef-2 Reporter Image Analysis. Images were captured on an Olympus BX61 epifluorescence compound microscope with a Hamamatsu ORCA-ER camera using Slidebook 4.0.1 digital microscopy software (Intelligent Imaging Innovations) and processed in ImageJ with custom scripts.

Dauer Induction and Postdauer Phenotyping. Dauer induction was achieved using crude dauer pheromone (81) for *kin-3* RNAi experiments and by starvation/crowding for experiments with *cgh-1*(*tn691*); *let-7*(*mg279*). All strains were maintained at 20 °C. Strains in the *cgh-1*(*tn691*); *let-7*(*mg279*) background were shifted to 25 °C at the L2 molt during continuous development or after selection of dauer larvae for postdauer development. Additional phenotyping details are provided in *SI Appendix, Supplemental Materials and Methods*.

CK2 in Vitro Kinase Assays. Recombinant GST fusion proteins were generated and isolated from *Escherichia coli* (82). Purified recombinant proteins were analyzed by SDS/PAGE and Coomassie Blue to determine protein concentrations by comparison with BSA standards. For in vitro kinase reactions, 1 μg of recombinant CGH-1 was mixed with 500 nM recombinant KIN-3 (either WT or K67M mutant), 500 nM KIN-10, 4 μCi of ^{32}P γATP, and 200 μM cold ATP in 20 mM Tris·HCl, pH 7.5, 50 mM KCl, and 20 mM MgCl2. Reactions were incubated at room temperature for 30 min. To inhibit CK2 activity in vitro, TBB was added to 5 μM. To map the specific phosphorylation site on CGH-1, GST-tagged CGH-1 peptides composed of the 20 aa flanking the four putative CK2 phosphorylation sites were incubated with CK2 as described above (peptide sequences in *SI Appendix*, Table S8). All data were analyzed by SDS/PAGE and autoradiography.

Western Blotting. Protein samples from synchronized populations were prepared by direct boiling in Novex Tris-glycine SDS sample buffer (Invitrogen), supplemented with 0.1 M DTT, resolved on Novex Tris-glycine gels (Invitrogen), and immobilized on Immobilon-FL transfer membrane (Millipore). Membranes were probed with custom rabbit polyclonal antibodies to ALG-1 (1:1,000), AIN-1 (1:1,000), CGH-1 (1:1,000), GFP (1:500), KIN-3 (1:500), TSN-1 (1:1,000), and VIG-1 (1:1,000), or γ-tubulin (Sigma LL-17) (1:2,000). Peroxidase-AffiniPure goat anti-rabbit IgG secondary antibody was used at 1:10,000 (Jackson ImmunoResearch Laboratories) for detection using Pierce ECL Western blotting substrate (Thermo Scientific).

Antibody Production. Custom polyclonal antibodies to *C. elegans* proteins were generated by immunizing rabbits with synthetic antigenic peptides conjugated to KLH (Proteintech). Antigenic peptide sequences are listed in *SI Appendix*, Table S8. Antibody to GFP was made using recombinant GFP purified from *E. coli*. The LIN-14 antibody was a gift from Gary Ruvkun, Department of Molecular Biology, Massachusetts General Hospital, Boston (83).

Immunoprecipitation and Mass Spectrometry. Synchronized populations were frozen in liquid nitrogen and homogenized with a Mixer Mill MM 400 ball mill homogenizer (Retsch). Immunoprecipitations from homogenates were performed using guidelines described (84). AIN-1 mass spectrometry was performed, in duplicate, on complexes isolated using a housemade AIN-1 antibody in gravid wild-type (N2) and *ain-1*(*tm3681*) samples. CGH-1 mass spectrometry was performed on complexes isolated using an endogenous CGH-1 antibody in L3 and adult wild-type (N2) worms. CGH-1 phosphoproteomic analysis by mass spectrometry was performed on complexes isolated using an endogenous CGH-1 antibody in empty vector and *kin-3* RNAi-treated adult worms. Protein identification by mass spectrometry was performed as described (85). Additional details are provided in *SI Appendix, Supplemental Materials and Methods*.

RNA Analyses. Samples were collected from synchronized populations at the following times: 48 h post-L1 for mature miRNA, 44 h post-L1 for *lin-41* mRNA, and 40 h post-L1 *daf-12* mRNA. Biological replicates for let-7 target analysis indicate at least two samples for which animal collection, RNA extraction, and qPCR analysis were conducted independently. Conditions for *kin-3*, *kin-10*, and *alg-1* RNAi are described in *SI Appendix, Supplemental Materials and Methods, Modified RNAi Conditions*. Total RNA isolation was conducted as described (86). For miRNA analysis: (*i*) Northern blotting was

performed as described (87) using 1.5 μg total RNA and Starfire DNA probes (IDT) (*SI Appendix*, Table S8), and (*ii*) RT-qPCR analysis was conducted using miRNA TaqMan assays and probes (hsa-let-7a, cat. no. 4427975; cel-miR-48, cat. no. 4427975; and U18, cat. no. 4427975) (Applied Biosystems) as described (86). For mRNA analysis, cDNA was synthesized from total RNA using the Multiscribe Reverse Transcriptase Kit (Applied Biosystems). Specific mRNAs were analyzed by RT-qPCR using Power SYBR Green Master Mix 2X (Applied Biosystems). Relative miRNA and mRNA levels were calculated based on the ΔΔ2Ct method (88) using U18 and *eft-2* for normalization, respectively. RT-qPCR primer sequences and Starfire Probes are listed in *SI Appendix*, Table S8).

RIP. GFP–ALG-1 was immunoprecipitated from L4 stage (48 h post-L1) CT20 with 3E6 anti-GFP antibody (Invitrogen). For each RIP, antibody was cross-linked to Protein A Dynabeads (Invitrogen) and incubated at 4 °C for 1 h with homogenized sample. Beads were washed with RIP wash buffer (50 mM Tris·HCl pH 7.5, 200 mM KCl, 0.05% Nonidet P-40), then split for protein and RNA analyses. For protein analyses, SDS sample buffer (Novex Tris-glycine; Invitrogen), was added directly to beads and incubated at 50 °C for 10 min. Eluted proteins were supplemented with 0.1 M DTT and incubated at 90 °C for 5 min before Western blotting. For RNA analysis, 1 mL of TRI-Reagent (Ambion) and 10 ng of Firefly Luciferase RNA (Promega) were directly added to beads and extracted as described in "RNA Analyses," with extended RNA precipitation for 2 h at −30 °C. cDNA and miRNA taqmans were synthesized and analyzed as described in "RNA Analyses." RT-qPCR analyses were normalized to Firefly Luciferase.

Small RNA Sequencing and miRNA Analysis. Samples were collected from synchronized populations of 48 h postarrested L1 fed L4440, *kin-3*, or *kin-10* RNAi. Total RNA was isolated as described in the "RNA Analyses" section. Total RNA was submitted to the Beijing Genomics Institute (BGI) for deep sequencing. Sequencing reads were processed to remove low-quality reads and trim artificial adapter sequences following BGI protocols. Briefly, reads were marked and removed for low quality if they had (*i*) more than four bases whose quality score was lower than 10 or (*ii*) more than six bases whose quality score was lower than 13. The 3′ adapter sequences were then trimmed from the remaining high-quality reads. Finally, reads were removed if they (*i*) lacked a 3′ adapter sequence, (*ii*) were 5′–3′ adapter ligation products, (*iii*) were 5′–5′ adapter ligation products, (*iv*) were shorter than 18 nt, or (*v*) contained only As (homopolymers). High-quality reads were aligned to the reference *C. elegans* genome version WS220 using Bowtie2 (89) with the following parameters: -f -N 0 -M 10. Reads that aligned with zero mismatches to one genomic locus were annotated to mature miRNA coordinates from miRBase Release 19 (4). Mature miRNA read counts in each library were normalized to the number of mapped reads in the library; mature miRNA abundance is reported as reads per million (RPM) mapped reads (*SI Appendix*, Table S4). Raw sequence data are available through the NCBI's Gene Expression Omnibus using accession GSE66764.

ACKNOWLEDGMENTS. We thank Ken Inoki, Patrick Hu, and Alison Frand for discussions; Natasha Weiser for manuscript editing; Dawen Cai for custom scripts used to analyze images in ImageJ; and Gary Ruvkun for the LIN-14 antibody. Indicated strains were provided by the *Caenorhabditis* Genetics Center, which is funded by the NIH Office of Research Infrastructure Programs (P40 OD010440). This work was also supported by grants from the American Cancer Society (RSG RMC-125264) and NIH (GM088565) (to J.K.K.), National Center for Research Resources (5P41RR011823) and NIH (8 P41 GM103533) (to J.R.Y.), and an Early Career Grant (C62241) from Central Michigan University (to X.K.).

1. Reinhart BJ, et al. (2000) The 21-nucleotide let-7 RNA regulates developmental timing in Caenorhabditis elegans. *Nature* 403(6772):901–906.
2. Lee RC, Feinbaum RL, Ambros V (1993) The C. elegans heterochronic gene lin-4 encodes small RNAs with antisense complementarity to lin-14. *Cell* 75(5):843–854.
3. Bartel DP (2009) MicroRNAs: Target recognition and regulatory functions. *Cell* 136(2): 215–233.
4. Griffiths-Jones S, Grocock RJ, van Dongen S, Bateman A, Enright AJ (2006) miRBase: microRNA sequences, targets and gene nomenclature. *Nucleic Acids Res* 34(Database issue):D140–D144.
5. Friedman RC, Farh KK, Burge CB, Bartel DP (2009) Most mammalian mRNAs are conserved targets of microRNAs. *Genome Res* 19(1):92–105.
6. Kim VN (2005) MicroRNA biogenesis: Coordinated cropping and dicing. *Nat Rev Mol Cell Biol* 6(5):376–385.
7. Kim VN, Han J, Siomi MC (2009) Biogenesis of small RNAs in animals. *Nat Rev Mol Cell Biol* 10(2):126–139.
8. Huntzinger E, Izaurralde E (2011) Gene silencing by microRNAs: Contributions of translational repression and mRNA decay. *Nat Rev Genet* 12(2):99–110.
9. Grishok A, et al. (2001) Genes and mechanisms related to RNA interference regulate expression of the small temporal RNAs that control C. elegans developmental timing. *Cell* 106(1):23–34.
10. Tops BB, Plasterk RH, Ketting RF (2006) The Caenorhabditis elegans Argonautes ALG-1 and ALG-2: almost identical yet different. *Cold Spring Harb Symp Quant Biol* 71: 189–194.
11. Ding L, Spencer A, Morita K, Han M (2005) The developmental timing regulator AIN-1 interacts with miRISCs and may target the argonaute protein ALG-1 to cytoplasmic P bodies in C. elegans. *Mol Cell* 19(4):437–447.
12. Zhang L, et al. (2007) Systematic identification of C. elegans miRISC proteins, miRNAs, and mRNA targets by their interactions with GW182 proteins AIN-1 and AIN-2. *Mol Cell* 28(4):598–613.
13. Rajyaguru P, Parker R (2009) CGH-1 and the control of maternal mRNAs. *Trends Cell Biol* 19(1):24–28.
14. Boag PR, Atalay A, Robida S, Reinke V, Blackwell TK (2008) Protection of specific maternal messenger RNAs by the P body protein CGH-1 (Dhh1/RCK) during Caenorhabditis elegans oogenesis. *J Cell Biol* 182(3):543–557.
15. Hammell CM, Lubin I, Boag PR, Blackwell TK, Ambros V (2009) nhl-2 Modulates microRNA activity in Caenorhabditis elegans. *Cell* 136(5):926–938.
16. Rouya C, et al. (2014) Human DDX6 effects miRNA-mediated gene silencing via direct binding to CNOT1. *RNA* 20(9):1398–1409.
17. Mathys H, et al. (2014) Structural and biochemical insights to the role of the CCR4-NOT complex and DDX6 ATPase in microRNA repression. *Mol Cell* 54(5):751–765.
18. Chen Y, et al. (2014) A DDX6-CNOT1 complex and W-binding pockets in CNOT9 reveal direct links between miRNA target recognition and silencing. *Mol Cell* 54(5):737–750.
19. Caudy AA, et al. (2003) A micrococcal nuclease homologue in RNAi effector complexes. *Nature* 425(6956):411–414.
20. Wilczynska A, Bushell M (2015) The complexity of miRNA-mediated repression. *Cell Death Differ* 22(1):22–33.
21. Kim YK, Heo I, Kim VN (2010) Modifications of small RNAs and their associated proteins. *Cell* 143(5):703–709.
22. Qi HH, et al. (2008) Prolyl 4-hydroxylation regulates Argonaute 2 stability. *Nature* 455(7211):421–424.
23. Zeng Y, Sankala H, Zhang X, Graves PR (2008) Phosphorylation of Argonaute 2 at serine-387 facilitates its localization to processing bodies. *Biochem J* 413(3):429–436.
24. Rybak A, et al. (2009) The let-7 target gene mouse lin-41 is a stem cell specific E3 ubiquitin ligase for the miRNA pathway protein Ago2. *Nat Cell Biol* 11(12):1411–1420.
25. Rüdel S, et al. (2011) Phosphorylation of human Argonaute proteins affects small RNA binding. *Nucleic Acids Res* 39(6):2330–2343.
26. Sahin U, Lapaquette P, Andrieux A, Faure G, Dejean A (2014) Sumoylation of human argonaute 2 at lysine-402 regulates its stability. *PLoS One* 9(7):e102957.
27. Wulczyn FG, Cuevas E, Franzoni E, Rybak A (2011) miRNAs need a Trim: Regulation of miRNA activity by Trim-NHL proteins. *Adv Exp Med Biol* 700:85–105.
28. Schwamborn JC, Berezikov E, Knoblich JA (2009) The TRIM-NHL protein TRIM32 activates microRNAs and prevents self-renewal in mouse neural progenitors. *Cell* 136(5): 913–925.
29. Huang KL, Chadee AB, Chen CY, Zhang Y, Shyu AB (2013) Phosphorylation at intrinsically disordered regions of PAM2 motif-containing proteins modulates their interactions with PABPC1 and influences mRNA fate. *RNA* 19(3):295–305.
30. Shen J, et al. (2013) EGFR modulates microRNA maturation in response to hypoxia through phosphorylation of AGO2. *Nature* 497(7449):383–387.
31. Kim JK, et al. (2005) Functional genomic analysis of RNA interference in C. elegans. *Science* 308(5725):1164–1167.
32. Tabach Y, et al. (2013) Identification of small RNA pathway genes using patterns of phylogenetic conservation and divergence. *Nature* 493(7434):694–698.
33. Niefind K, Raaf J, Issinger OG (2009) Protein kinase CK2 in health and disease: Protein kinase CK2: From structures to insights. *Cell Mol Life Sci* 66(11–12):1800–1816.
34. Hu E, Rubin CS (1990) Casein kinase II from Caenorhabditis elegans. Properties and developmental regulation of the enzyme; cloning and sequence analyses of cDNA and the gene for the catalytic subunit. *J Biol Chem* 265(9):5072–5080.
35. Abbott AL, et al. (2005) The let-7 MicroRNA family members mir-48, mir-84, and mir-241 function together to regulate developmental timing in Caenorhabditis elegans. *Dev Cell* 9(3):403–414.
36. Sulston JE, Horvitz HR (1977) Post-embryonic cell lineages of the nematode, Caenorhabditis elegans. *Dev Biol* 56(1):110–156.
37. Koh K, Rothman JH (2001) ELT-5 and ELT-6 are required continuously to regulate epidermal seam cell differentiation and cell fusion in C. elegans. *Development* 128(15):2867–2880.
38. Liu Z, Kirch S, Ambros V (1995) The Caenorhabditis elegans heterochronic gene pathway controls stage-specific transcription of collagen genes. *Development* 121(8): 2471–2478.
39. Abrahante JE, Miller EA, Rougvie AE (1998) Identification of heterochronic mutants in Caenorhabditis elegans. Temporal misexpression of a collagen:green fluorescent protein fusion gene. *Genetics* 149(3):1335–1351.
40. Hayes GD, Frand AR, Ruvkun G (2006) The mir-84 and let-7 paralogous microRNA genes of Caenorhabditis elegans direct the cessation of molting via the conserved nuclear hormone receptors NHR-23 and NHR-25. *Development* 133(23):4631–4641.
41. Ecsedi M, Rausch M, Großhans H (2015) The let-7 microRNA directs vulval development through a single target. *Dev Cell* 32(3):335–344.
42. Johnson SM, et al. (2005) RAS is regulated by the let-7 microRNA family. *Cell* 120(5): 635–647.
43. Sternberg PW (2005) Vulval development. *WormBook* 1–28.

44. Eisenmann DM, Kim SK (1997) Mechanism of activation of the Caenorhabditis elegans ras homologue let-60 by a novel, temperature-sensitive, gain-of-function mutation. *Genetics* 146(2):553–565.
45. Johnston RJ, Hobert O (2003) A microRNA controlling left/right neuronal asymmetry in Caenorhabditis elegans. *Nature* 426(6968):845–849.
46. Kennedy S, Wang D, Ruvkun G (2004) A conserved siRNA-degrading RNase negatively regulates RNA interference in C. elegans. *Nature* 427(6975):645–649.
47. Schmitz C, Kinge P, Hutter H (2007) Axon guidance genes identified in a large-scale RNAi screen using the RNAi-hypersensitive Caenorhabditis elegans strain nre-1(hd20) lin-15b(hd126). *Proc Natl Acad Sci USA* 104(3):834–839.
48. Sarin S, et al. (2007) Genetic screens for Caenorhabditis elegans mutants defective in left/right asymmetric neuronal fate specification. *Genetics* 176(4):2109–2130.
49. Alvarez-Saavedra E, Horvitz HR (2010) Many families of C. elegans microRNAs are not essential for development or viability. *Curr Biol* 20(4):367–373.
50. Slack FJ, et al. (2000) The lin-41 RBCC gene acts in the C. elegans heterochronic pathway between the let-7 regulatory RNA and the LIN-29 transcription factor. *Mol Cell* 5(4):659–669.
51. Bagga S, et al. (2005) Regulation by let-7 and lin-4 miRNAs results in target mRNA degradation. *Cell* 122(4):553–563.
52. Lin YC, et al. (2007) Human TRIM71 and its nematode homologue are targets of let-7 microRNA and its zebrafish orthologue is essential for development. *Mol Biol Evol* 24(11):2525–2534.
53. Ding XC, Grosshans H (2009) Repression of C. elegans microRNA targets at the initiation level of translation requires GW182 proteins. *EMBO J* 28(3):213–222.
54. Wightman B, Ha I, Ruvkun G (1993) Posttranscriptional regulation of the heterochronic gene lin-14 by lin-4 mediates temporal pattern formation in C. elegans. *Cell* 75(5):855–862.
55. Simon DJ, et al. (2008) The microRNA miR-1 regulates a MEF-2-dependent retrograde signal at neuromuscular junctions. *Cell* 133(5):903–915.
56. Chan SP, Slack FJ (2009) Ribosomal protein RPS-14 modulates let-7 microRNA function in Caenorhabditis elegans. *Dev Biol* 334(1):152–160.
57. Zielinska DF, Gnad F, Jedrusik-Bode M, Wiśniewski JR, Mann M (2009) Caenorhabditis elegans has a phosphoproteome atypical for metazoans that is enriched in developmental and sex determination proteins. *J Proteome Res* 8(8):4039–4049.
58. Yochem J, Greenwald I (1989) glp-1 and lin-12, genes implicated in distinct cell-cell interactions in C. elegans, encode similar transmembrane proteins. *Cell* 58(3):553–563.
59. Austin J, Kimble J (1987) glp-1 is required in the germ line for regulation of the decision between mitosis and meiosis in C. elegans. *Cell* 51(4):589–599.
60. Dosztányi Z, Csizmok V, Tompa P, Simon I (2005) IUPred: Web server for the prediction of intrinsically unstructured regions of proteins based on estimated energy content. *Bioinformatics* 21(16):3433–3434.
61. Collins MO, Yu L, Campuzano I, Grant SG, Choudhary JS (2008) Phosphoproteomic analysis of the mouse brain cytosol reveals a predominance of protein phosphorylation in regions of intrinsic sequence disorder. *Mol Cell Proteomics* 7(7):1331–1348.
62. Gnad F, Gunawardena J, Mann M (2011) PHOSIDA 2011: The posttranslational modification database. *Nucleic Acids Res* 39(Database issue):D253–D260.
63. Gnad F, et al. (2007) PHOSIDA (phosphorylation site database): Management, structural and evolutionary investigation, and prediction of phosphosites. *Genome Biol* 8(11):R250.
64. Scheckel C, Gaidatzis D, Wright JE, Ciosk R (2012) Genome-wide analysis of GLD-1-mediated mRNA regulation suggests a role in mRNA storage. *PLoS Genet* 8(5): e1002742.
65. Cassada RC, Russell RL (1975) The dauerlarva, a post-embryonic developmental variant of the nematode Caenorhabditis elegans. *Dev Biol* 46(2):326–342.
66. Liu Z, Ambros V (1991) Alternative temporal control systems for hypodermal cell differentiation in Caenorhabditis elegans. *Nature* 350(6314):162–165.
67. Euling S, Ambros V (1996) Reversal of cell fate determination in Caenorhabditis elegans vulval development. *Development* 122(8):2507–2515.
68. Karp X, Ambros V (2012) Dauer larva quiescence alters the circuitry of microRNA pathways regulating cell fate progression in C. elegans. *Development* 139(12): 2177–2186.
69. Poole A, et al. (2005) A global view of CK2 function and regulation. *Mol Cell Biochem* 274(1–2):163–170.
70. Hubstenberger A, Noble SL, Cameron C, Evans TC (2013) Translation repressors, an RNA helicase, and developmental cues control RNP phase transitions during early development. *Dev Cell* 27(2):161–173.
71. Wang JT, et al. (2014) Regulation of RNA granule dynamics by phosphorylation of serine-rich, intrinsically disordered proteins in C. elegans. *eLife* 3:e04591.
72. Castello A, et al. (2012) Insights into RNA biology from an atlas of mammalian mRNA-binding proteins. *Cell* 149(6):1393–1406.
73. Brangwynne CP (2013) Phase transitions and size scaling of membrane-less organelles. *J Cell Biol* 203(6):875–881.
74. Han TW, et al. (2012) Cell-free formation of RNA granules: Bound RNAs identify features and components of cellular assemblies. *Cell* 149(4):768–779.
75. Kato M, et al. (2012) Cell-free formation of RNA granules: Low complexity sequence domains form dynamic fibers within hydrogels. *Cell* 149(4):753–767.
76. Mitchell SF, Parker R (2014) Principles and properties of eukaryotic mRNPs. *Mol Cell* 54(4):547–558.
77. Stiernagle T (2006) Maintenance of C. elegans. *WormBook* 1–11.
78. Fraser AG, et al. (2000) Functional genomic analysis of C. elegans chromosome I by systematic RNA interference. *Nature* 408(6810):325–330.
79. Rual JF, et al. (2004) Toward improving Caenorhabditis elegans phenome mapping with an ORFeome-based RNAi library. *Genome Res* 14(10B):2162–2168.
80. Kamath RS, Ahringer J (2003) Genome-wide RNAi screening in Caenorhabditis elegans. *Methods* 30(4):313–321.
81. Vowels JJ, Thomas JH (1994) Multiple chemosensory defects in daf-11 and daf-21 mutants of Caenorhabditis elegans. *Genetics* 138(2):303–316.
82. Harper S, Speicher DW (2011) Purification of proteins fused to glutathione S-transferase. *Methods Mol Biol* 681:259–280.
83. Reinhart BJ, Ruvkun G (2001) Isoform-specific mutations in the Caenorhabditis elegans heterochronic gene lin-14 affect stage-specific patterning. *Genetics* 157(1): 199–209.
84. Zanin E, et al. (2011) Affinity purification of protein complexes in C. elegans. *Methods Cell Biol* 106:289–322.
85. Gu W, et al. (2009) Distinct argonaute-mediated 22G-RNA pathways direct genome surveillance in the C. elegans germline. *Mol Cell* 36(2):231–244.
86. Billi AC, et al. (2012) The Caenorhabditis elegans HEN1 ortholog, HENN-1, methylates and stabilizes select subclasses of germline small RNAs. *PLoS Genet* 8(4):e1002617.
87. Pall GS, Codony-Servat C, Byrne J, Ritchie L, Hamilton A (2007) Carbodiimide-mediated cross-linking of RNA to nylon membranes improves the detection of siRNA, miRNA and piRNA by northern blot. *Nucleic Acids Res* 35(8):e60.
88. Nolan T, Hands RE, Bustin SA (2006) Quantification of mRNA using real-time RT-PCR. *Nat Protoc* 1(3):1559–1582.
89. Langmead B, Salzberg SL (2012) Fast gapped-read alignment with Bowtie 2. *Nat Methods* 9(4):357–359.